Title
Transport of Vacuum Arc Plasma Through Straight and Curved Magnetic Ducts

Journal
Journal of applied physics, 66(11)

Authors
Storer, J.
Galvin, J.E.
Brown, I.G.

Publication Date
2017-11-29

LBL-27112
Preprint

Lawrence Berkeley Laboratory
UNIVERSITY OF CALIFORNIA

Accelerator & Fusion Research Division

Submitted to Journal of Applied Physics

Transport of Vacuum Arc Plasma through Straight and Curved Magnetic Ducts

J. Storer, J.E. Galvin, and I.G. Brown

April 1989

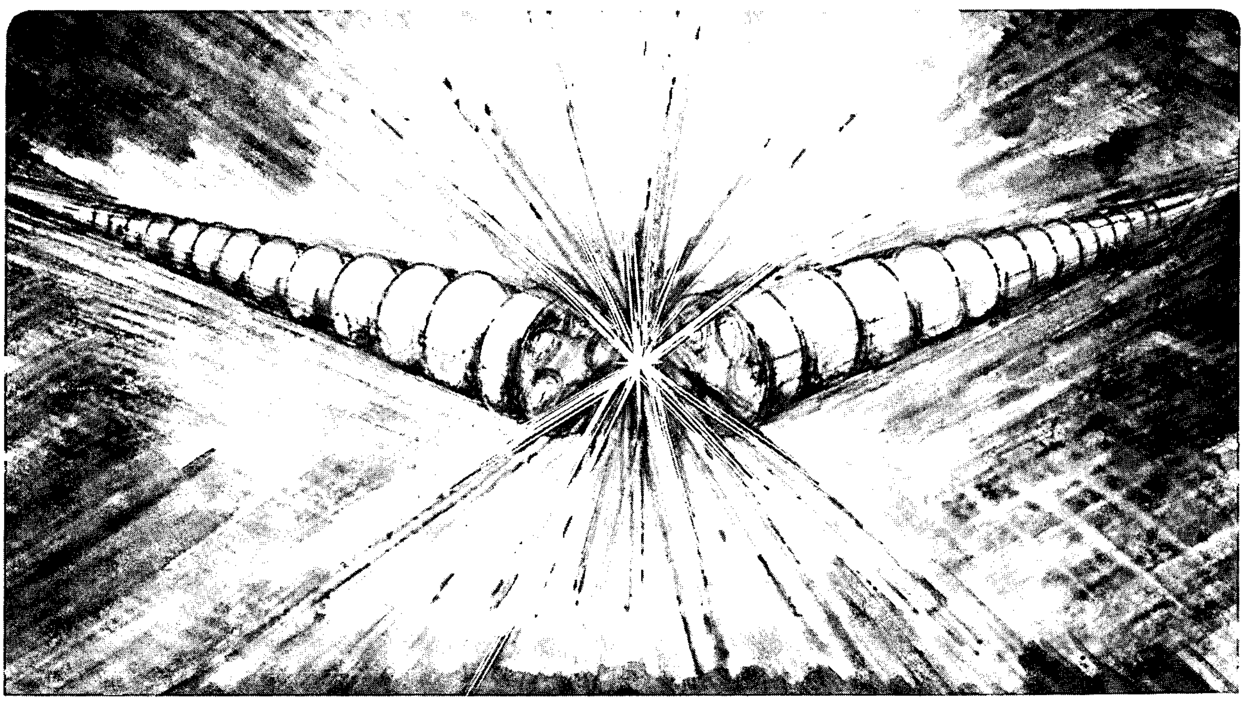

Prepared for the U.S. Department of Energy under Contract Number DE-AC03-76SF00098.

LBL-27112

TRANSPORT OF VACUUM ARC PLASMA THROUGH STRAIGHT AND CURVED MAGNETIC DUCTS*

J. Storer
3M
St. Paul, MN 55144

and

J. E. Galvin and I. G. Brown
Lawrence Berkeley Laboratory
University of California
Berkeley, CA 94720

April, 1989

* Supported by the Director, Office of Energy Research, Office of High Energy and Nuclear Physics, Nuclear Science Division, U.S. Department of Energy under Contract No. DE-AC03-76SF00098, and by the U.S. DOE Industry-Laboratory Technology Exchange Program.

TRANSPORT OF VACUUM ARC PLASMA THROUGH STRAIGHT AND CURVED MAGNETIC DUCTS*

J. Storer
3M
St. Paul, MN 55144

and

J. E. Galvin and I. G. Brown
Lawrence Berkeley Laboratory
University of California
Berkeley, CA 94720

April, 1989

ABSTRACT

We report on an experimental investigation of the transport of a metal vapor vacuum arc plasma through straight and curved magnetic solenoids for the case of an iron plasma and for magnetic field strength up to 650 Gauss. We find that the fraction of plasma transported increases with magnetic field strength and saturates at a field at which the ion gyroradius equals the radius of the plasma channel. The magnetic field strength at the cathode location, where the plasma is injected into the solenoid, was found to be important, and for the present work the injection efficiency optimizes at a field of about 150 Gauss.

I. INTRODUCTION

Vacuum arc plasma sources are attractive devices for the deposition of metallic thin films [1-3]. These kinds of sources produce intense fluxes of highly ionized metal plasmas which when condensed form highly adherent and dense thin films. However, they suffer from a severe limitation: along with the metal plasma that is generated there is also a flux of macroscopic droplets, of size typically in the broad range 0.1 - 10 microns [4-8]. The origin of these macroparticles is at the cathode spot itself and results from the intense heating of the cathode material beneath the spot [9]. A volume of material is rendered molten by the arc and the pressure gradient in the vicinity of the arc expels molten droplets along with the vapor. The volume of molten material formed by the arc's heating is less for higher melting point materials, and the macroparticle contamination is observed to be less for cathode materials of higher melting point. For some applications, useful films can be made by proper selection of cathode material. In the case of a carbon cathode (and also some other elements and compounds), even larger solid particles are ejected from the arc spot. These result from the porous nature of most solid carbon materials. Gas trapped in voids in the cathode causes pressure gradients which blow solid pieces of cathode from the source. It is also possible that small bridges between grains of the source material are broken by extreme compressive stress, leading to particle ejection [10].

The application base for vacuum arc sources could be widened substantially if the macroparticles either could be stopped from forming or if they could be filtered out of the plasma stream, and several workers have reported on devices and operational procedures for macroparticle removal [11-17]. The macroparticles travel in approximately straight line trajectories from the cathode because their velocities are quite high, up to 800 m/sec [18-19]. An effective filter could thus be an optically dense channel which permits plasma transmission with good efficiency. One simple configuration is a curved tube or pipe which precludes line-of-sight macroparticles from passing through it, while allowing a relatively high transmission of plasma by virtue of an axial magnetic field which ducts the plasma through the filter [11,12,20-22]. Loss of plasma through the filter results in a decrease in deposition rate at the other end.

In the work described here we have carried out a series of experiments to investigate transport of the metal plasma through such a magnetic filter. The cathode material used was type 304 stainless steel (Fe70%/Cr20%/Ni10%). The spatial distribution of the plasma loss through the filter and the dependence of the transport efficiency on magnetic field intensity were measured. Various other characteristics of this kind of magnetic filter were also studied, such as the dependence of the plasma transport on the wall potential, and means of efficiently injecting plasma into the magnetic duct.

II. EXPERIMENTAL SET-UP

Two different plasma ducts were used for these measurements. One duct, suitable as a filter, was curved and the other, for comparison, was straight. Their length was 22 cm and the inner diameter of the plasma transport channel (see below) was 3.05 cm. The 90° bend of the curved duct did not allow any line-of-sight trajectories from the cathode to the far end, and therefore no macroparticles could pass through it unless they had been reflected from the filter's interior. Photographs of the two ducts are shown in Figure 1.

The magnetic field was established by a solenoid wound from copper tubing through which water was passed for cooling. The solenoid consisted of 25 turns of 4.75 mm o.d. tubing wound with an average turn-to-turn spacing of 8.9 mm and an i.d. of 4.6 cm. Both ducts - the straight and the curved - were made the same in all ways apart from the curvature, so that the results would be comparable. The maximum dc magnetic field that could be obtained (cooling limited) in these experiments was 650 Gauss.

The inner wall of the two ducts consisted of aluminum disks with sharpened inner edges. The disks served several separate purposes: (i) they provided a well-defined and controllable plasma boundary, (ii) they provided a shield between the plasma stream and the magnetic field solenoid, and (iii) they reduced the probability of macroparticle transport through the duct via reflections from the walls. The inside diameter of the disks was 3.05 cm, and their on-axis separation was 1 cm. They were isolated electrically and it was possible to connect them to either of the electrodes (anode or cathode), float them, ground them, or put them at an arbitrary potential with respect to ground.

The plasma generator ("plasma gun") was a simple metal vapor vacuum arc plasma source of the type developed for the MEVVA series of high current metal ion sources [23-25]. It consists of a 0.63 cm diameter cathode and a tubular anode. A small trigger electrode surrounds the cathode coaxially and is separated from it by an alumina insulator. The arc is initiated by applying a short (several microseconds) high voltage (several kV) trigger pulse to the trigger electrode. A surface discharge across the alumina insulator, between trigger electrode and cathode, generates a small amount of plasma which bridges the anode-cathode gap and allows the main arc current to flow. The arc current is supplied by an L-C pulse line of length 250 microseconds and impedance 1 Ohm. Thus, our experimental device operates in a pulse mode (although the magnetic field is on d.c.). The anode of the plasma gun was held at ground potential. The plasma gun assembly can be seen in Fig. 1; it can be moved along the duct axis. The properties of the plasma generated by this kind of plasma gun, as reflected in the extracted ion beam, have been extensively studied as part of the LBL MEVVA ion source R&D program. The MEVVA ion source has been fully described elsewhere [23-26].

The ion current was measured by a biased probe which could be moved along the duct axis from outside the vacuum vessel. Thus the fall-off in ion current with distance from the source in each of the two ducts, straight and curved, could be measured for a given set of parameters. The probe itself was a disk of 2.54 cm diameter attached to the end of the probe support mechanism; the probe (current collector) was thus a reasonably tight fit to the inner diameter of the aluminum disks forming the wall of the duct (3.05 cm i.d.). The probe was biased at a potential of -70 V with respect to the plasma (the anode of the plasma gun was grounded) so as to be in the ion saturation region of the probe characteristic [27,28]; that the probe bias was appropriate for ion collection was checked from time to time by varying the bias voltage to ensure that the ion collection signal was indeed in the saturation region. The probe signal can be thought of as a measure of the ion flux available for deposition at that particular location in the duct or as the plasma density at that location. The ion current measured in this way was cross-checked for some cases by comparison with another technique involving the shift in resonant frequency of a small piezo-electric crystal [29,30].

III. RESULTS

As described above, the mass transport along the magnetic duct was measured in two different ways - by the ion saturation current collected by a negatively biased circular collector plate, and by the change in resonant frequency of a small quartz crystal caused by the increase of mass on the crystal surface. By using the quartz crystal as the current collector as well as a microbalance, (ie, replacing the circular current collector plate by the crystal), we could make a direct comparison of the two methods. the results of this comparison are shown in Fig. 2. Here, the Δm_{xtal} has been obtained from the measured frequency shift, having first calibrated the crystal against a precisely measured mass increase. The $\Delta m_{current}$ has been obtained from the measured ion saturation current to the collector where the mean ion charge state has been taken as that given in reference 26. These data were provided by scanning in magnetic field strength and axial location of the probe, using the straight magnetic duct. The two methods agree well.

Our goal was to measure the intrinsic transmission of the two ducts. It was thus advantageous to always inject a fixed ion flux axially into the entrance of the duct under investigation. From previous work [28] it is known that the ion current projected in the forward direction by a magnetic field saturates at a maximum value which is determined only by the total arc current, and that this maximum ion current is achieved for a ducting magnetic field strength greater than only about 150 Gauss. Larger magnetic field strengths than this do not increase the saturation ion current, but in fact cause the arc to become unstable, in turn leading to arc ignition difficulties and erratic ion current measurements. In order to keep the magnetic field at the cathode at about 150 Gauss, independent of the duct field, a small solenoid ("minicoil") was positioned around the cathode and anode. The minicoil was of length 4.45 cm and inner diameter 2.54 cm and was positioned inside the duct solenoid. The minicoil magnetic field could either add to or subtract from the duct magnetic field, thus providing control over the magnetic field at the cathode independent of the duct magnetic field. A typical set of results showing the effect of the minicoil is shown in Figure 3. Here the magnetic field of the curved duct was kept at 650 Gauss and the minicoil magnetic field varied, while the ion saturation current collected by the disk probe located at the exit end of the duct was monitored. The best conditions - i.e., the most stable arc and highest ducted ion current at the exit - were achieved for a magnetic field strength at the cathode of about 150 Gauss. This mode of operation was then used throughout.

Axial profiles of the transported plasma flux for a range of magnetic field strengths are shown in Figures 4 and 5. Figure 4 shows the ion saturation current collected by the axially-moving probe as a function of distance from cathode to probe, for magnetic field strengths from 0 up to 650 gauss, for the straight magnetic duct, and Figure 5 shows similar data for the curved magnetic duct. Each of the fitted curves defines an attenuation length (the distance over which the plasma density falls by a factor of e), and this is plotted as a function of magnetic field strength in Figure 6. The attenuation length for both the straight and curved ducts increases with magnetic field strength and approaches an asymptotic value of about 16 cm for the straight duct and about 10 cm for the curved duct.

Plasma loss through the duct was investigated further by measuring the ion saturation current to each of the aluminum disks forming the duct wall. The curved duct was used with all the disks grounded (this gave the highest throughput) except for that one disk for which the ion saturation current was to be measured, which was biased to -70 V; all disks were monitored, one-by-one from the entrance of the duct to the exit. In this way the spatial distribution of the ion current to the duct wall (ie, the 'wall current') was determined. The results are shown in Figure 7. These data show that the axial fall-off of the wall current is the same as the axial fall-off of the ion saturation current measured by the axial moving probe. The total collected ion current - that measured by the probe plus the sum of the disk currents for all disks up to the probe location, for all probe locations - is a constant that depends only on the arc current; that is, all the current generated by the arc is accounted for. We ascribe the sharp initial drop in wall current to the detailed shape of the magnetic flux tube in the vicinity of the cathode due to the mini-coil surrounding the plasma gun.

We measured the location in the transverse plane of the ducted plasma channel by positioning a glass plate at the duct exit. For this experiment a copper cathode was used. The device was operated for a short time (about 1,500 shots) so as to build up a deposit on the glass. This was done for both the straight and the curved duct. The magnetic field was 650 Gauss. As expected, the deposition mark was located centrally for the case of the straight duct. For the curved duct the deposition mark was shifted out of the plane of the duct by approximately 0.5 cm. This effect could be due in part to curvature- and gradient-driven plasma drifts of the streaming plasma in the curved and non-uniform magnetic field [31-33].

Finally, we assembled a simple 'multipole magnetic duct' and measured the plasma transport through it. This device consisted of an iron pipe 22.9 cm long and 7.9 cm in inner diameter, with high-field samarium cobalt permanent magnets attached onto the inside surface of the pipe so as to form a long hexapole structure. The plasma channel diameter formed by the magnets was 3.9 cm. The measured plasma transmission through this structure was disappointedly low. Using the same axially scanning collector plate as used for the straight duct measurements described above, we measured a fraction of plasma transported over the 15.2 cm length of the multipole duct of only 7%.

IV. DISCUSSION

The two configurations of magnetic duct that we have investigated necessarily represent quite special cases in the range of parameter space over which it is conceptually possible to fabricate and operate magnetic ducts. Thus for example the absolute and relative magnitudes of important parameters such as duct length, duct major and minor radii, ion gyroradius, ion mean free path, among others, surely are important to the plasma transport through the duct, and we have been able to survey only a tiny part of this high-dimensional parameter space. The conclusions that we draw are therefore made very cautiously.

Plasma transport through the straight duct offers the least surprises. As can be seen from Figures 4 and 6, the transport efficiency increases with magnetic field strength and saturates at around 500 Gauss. The attenuation length of the plasma density along the duct is approximately equal to the inner radius of the duct for very low magnetic field, and increases to a saturation value at a magnetic field for which the ion gyroradius approximately equals the duct inner radius; (the ion temperature of the vacuum arc plasma has been taken to be of order 1 eV).

Interpretation of the observations of transport through the curved duct are more clouded. Certainly there is a greater plasma loss than in the straight duct, as is clear from Figure 6. The general behaviour seems to be similar to that for the straight duct in that the transport is minimal for low field strength (here less than a few hundred Gauss) and increases with field, possibly approaching a saturation value for $a/\rho_i > 1$, where a is the inner radius of the duct and ρ_i is the ion gyroradius. As mentioned above, measurements using a glass witness slide to show the gross position of the plasma channel at the end of the duct indicated that the plasma column was shifted out of the plane of the duct by up to about 0.5 cm at 650 Gauss; reversing the duct field polarity did not reverse the sense of the drift. This drift would cause a decrease in the ion current measured by the moveable collector plate since its diameter (2.54 cm) is less than the duct inner diameter (3.05 cm). The measured attenuation lengths thus include the effect of this gross loss also. We conclude that the curved duct investigated here is not optimized for plasma transport, and that major changes should be made, perhaps such as increasing the duct dimensions and hence a/ρ_i; it is possible that the addition of helical windings to the magnetic field configuration so as to produce a rotational transform in the field might help to alleviate the out-of-the-plane drift. We hope to investigate these things in future experiments.

There is a feature of the data shown in Figures 4 and 5 that is interesting to note. Of the several plots of ion saturation current as a function of distance along the magnetic duct, some show a noticeable departure from strict exponential fall-off. In taking the data we noticed these features and repeated the measurements several times; the features are repeatable. A similar phenomenon has recently been observed by Johnson, D'Angelo and Merlino [34]. These workers have studied the propagation of a low energy, charge neutralized ion beam in a long double plasma device in a magnetic field of up to about 180 Gauss - conditions generally similar to those employed in our work. They found that although the beam is mostly attenuated as it propagates downstream, under some conditions a "reemergence" of the beam on axis is observed. This effect was attributed to a focussing of the beam ions by a self-consistently produced radial ambipolar electric field. We speculate that the reproducible departures from strictly exponential fall-off seen in our data may be due to a similar or related effect.

V. CONCLUSION

We have measured the plasma transmission characteristics of two solenoidal magnetic plasma transport channels, one straight and one curved. The plasma used was that generated by a pulsed metal vapor vacuum arc plasma gun, and the magnetic field strength was varied over the range 0 - 650 Gauss.

We found that for the case of the straight duct the plasma transport efficiency, as measured by the attenuation length of the plasma density along the duct, increased with magnetic field strength up to a saturation value at a field strength for which the ion gyroradius is approximately equal to the duct radius. Transport through the curved duct was less, with a plasma density attenuation length roughly half of that for the straight duct. The magnetic field entrance condition was found to be important; there was an optimum field strength for coupling the maximum amount of plasma from the metal ion plasma generator into the duct, which for our configuration was about 150 Gauss.

ACKNOWLEDGEMENTS

We are indebted to Bob MacGill and Mark West for their support of the mechanical systems of the experimental facilities. This work was supported by the U.S. Department of Energy under Contract No. DE-AC03-76SF00098, and by a DOE National Laboratory - Industry Technology Transfer Program grant.

REFERENCES

1. R. L. Boxman, S. Goldsmith, S. Shalev, H. Yaloz and N. Brosh, Thin Solid Films 139, 41 (1985).
2. R. L. Boxman and S. Goldsmith, International Conference on Metallurgical Coatings, San Diego, CA, 23-27 March, 1986.
3. D. M. Sanders, J. Vac. Sci. Tech. A7, 2339 (1989).
4. T. Utsumi and J. H. English, J. Appl. Phys. 46, 126 (1974).
5. J. E. Daalder, J. Phys. D: Appl.Phys. 9, 2379 (1976).
6. D. T. Tuma, C. L. Chen and D. K. Davies, J. Appl. Phys. 49, 3821 (1978)
7. J. E. Daalder, Physica 104C, 91 (1981).
8. I. I. Aksenov, I. I. Konovalov, E. E. Kudryavtseva, V. V. Kunchenko, V. G. Padalka and V. M. Khoroshikh, Sov. Phys. Tech. Phys. 29(8), 893 (1984).
9. E. Hantzsche, 13th International Conference on Phenomena in Ionized Gases, Berlin, DDR, 1977.
10. H. Bolt, C. D. Croessman, A. Miyahara, T. Kuroda and Y. Oka, Institute of Plasma Physics, Nagoya University, Report IPPJ-AM-53, 1987.
11. I. I. Aksenov, V. A. Belous, V.G. Padalka and V. M. Khoroshikh, Sov. J. Plasma Phys. 4(4), 425 (1978).
12. I. I. Aksenov, V. A. Belous, V.G. Padalka and V. M. Khoroshikh, Instrum. and Exp. Techniques 21(5), 1416 (1978).
13. V. A. Osipov, V. G. Padalka, L. P. Sablev and R. I. Stupak, Instrum. and Exp. Techniques 21(6), 173 (1978).
14. I. I. Aksenov, S. I. Vakula, V. G. Padalka, V. E. Strelnitski and V. M. Khoroshikh, Sov. Phys. Tech. Phys. 25(9), 1164, (1980).
15. I. I. Axenov et al, U.S. Patent No. 4,452,686, June 5, 1984.
16. S. Ramalingam, International Patent WO 85/03954, 12 September 1985.
17. S. Boelens, H. Veltrop and H. Wesemeyer, International Conference on Metallurgical Coatings, San Diego, CA, March, 1987.
18. S. Shalev, R. L. Boxman and S. Goldsmith, J. Appl. Phys. 58, 2503 (1985).
19. S. Shalev and R. L. Boxman, IEEE Trans. Plasma Sci. PS-14, 59 (1986).
20. B. G. Safranov, V. S. Voitsenya and I. I. Konovalov, Sov. Phys. - Tech. Phys. 7(6), 495 (1962).
21. V. S. Voitsenya, A. G. Gorbanyuk, I. N. Onishchenko and B. G. Safranov, Sov. Phys. - Tech. Phys. 9(2), 221 (1964).
22. I. I. Aksenov, A. N. Belokhvostikov, V. G. Padalka, N. S. Repalov and V. M. Khoroshikh, Plasma Physics and Controlled Fusion 28, 761 (1986)
23. I. G. Brown, J. E. Galvin, and R. A. MacGill, Appl. Phys. Lett. 47, 358 (1985).
24. I. G. Brown, IEEE Trans. Nuc. Sci. NS-32, 1723 (1985).
25. I. G. Brown, J. E. Galvin, B. F. Gavin, and R. A. MacGill, Rev. Sci. Instrum. 57, 1069 (1986).
26. I. G. Brown, in "*The Physics and Technology of Ion Sources*," ed. I.G. Brown (Wiley, New York, 1989).
27. F. F. Chen, in "*Plasma Diagnostic Techniques*", ed. R. H. Huddlestone and S.L. Leonard, Academic Press, NY, 1965.
28. I. G. Brown, IEEE Trans. Plasma Sci. PS-15, 345 (1987)
29. C. Lu, J. Vac. Sci. Tech. 12, 578 (1975)
30. M. Moskovits and G.A. Ozin, in "*Cryochemistry*", edited by M. Moskovits and G. A. Ozin (Wiley, N.Y., 1976)
31. L. Spitzer, Jr., "*Physics of Fully Ionized Gases*" (Wiley, NY, 1965).
32. F. F. Chen, "*Introduction to Plasma Physics*" (Plenum, NY, 1974)

33. L. A. Artsimovich, "*A Physicist's ABC on Plasma*" (English translation, Mir Publishers, Moscow, 1978).
34. J. C. Johnson, N. D'Angelo and R. L. Merlino, IEEE Trans. Plasma Sci. PS-16, 590 (1988).

FIGURE CAPTIONS

Fig. 1. The two magnetic plasma ducts investigated: (a) straight and (b) curved. One can see the copper tubing solenoid, aluminum disks that define the plasma boundary, the plasma gun, and the probe movement mechanism; the plasma gun and the probe can be moved remotely.

Fig. 2. Transported mass measured by the quartz crystal oscillator frequency shift Δm_{xtal} vs. that obtained from the ion current collected by the probe $\Delta m_{current}$. The two methods are compared by varying the probe position and the magnetic field strength in the straight duct. The agreement is good.

Fig. 3. Ion saturation current measured at the duct exit vs. magnetic field at the cathode, for constant duct magnetic field, (the minicoil magnetic field was varied). Curved duct, B = 650 G.

Fig. 4. Plasma transport through the straight duct: ion saturation current to the probe as a function of probe position along the duct, for a range of magnetic field strengths.

Fig. 5. Plasma transport through the curved duct.

Fig. 6. Axial attenuation length of the plasma ion current as a function of magnetic field strength for straight and curved ducts

Fig. 7. Wall current as a function of distance along the duct. Curved duct, B = 650 Gauss. The fall-off in wall current is seen to be the same as that in the signal collected by the probe.

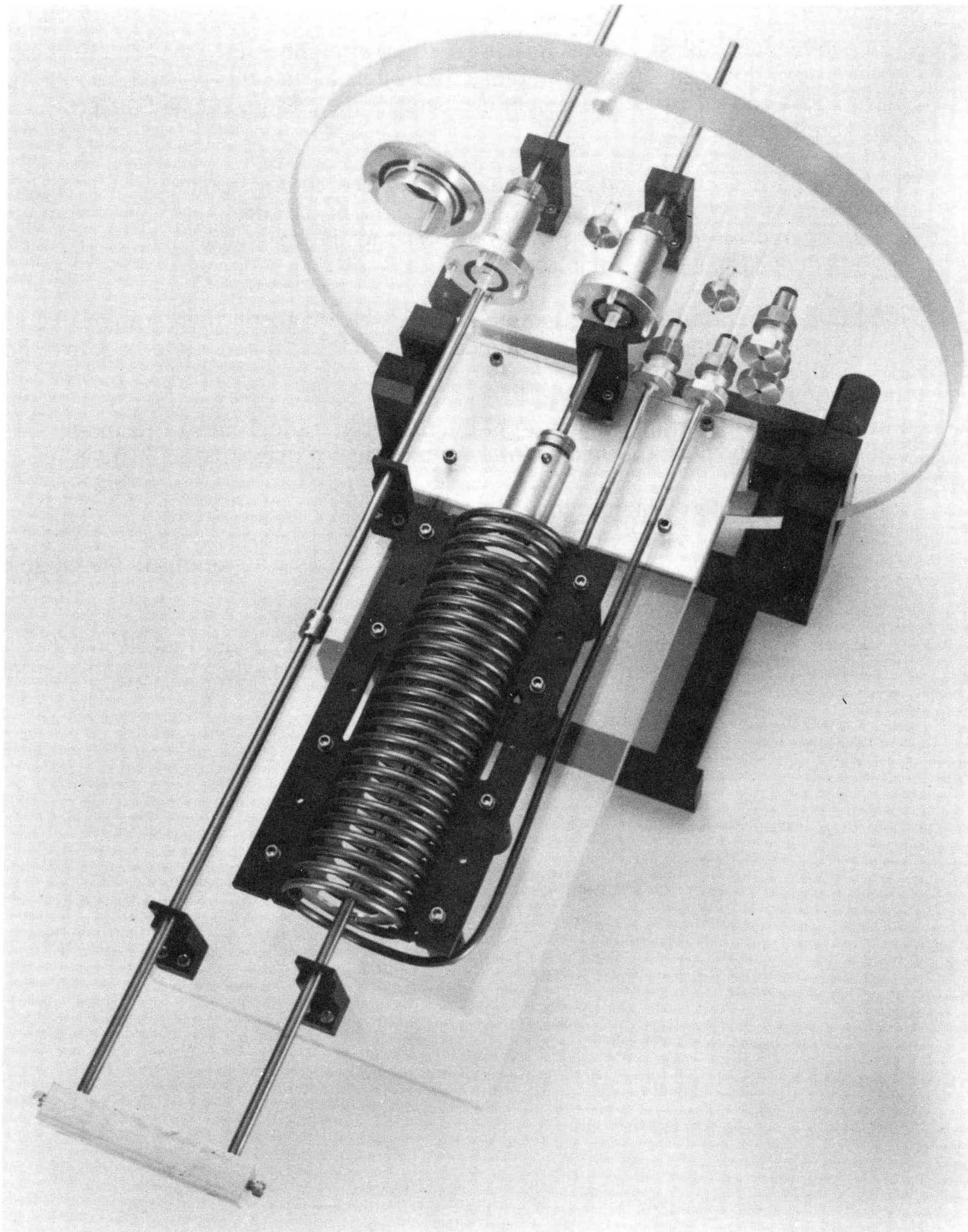

Figure 1(a)

CBB 887-6899

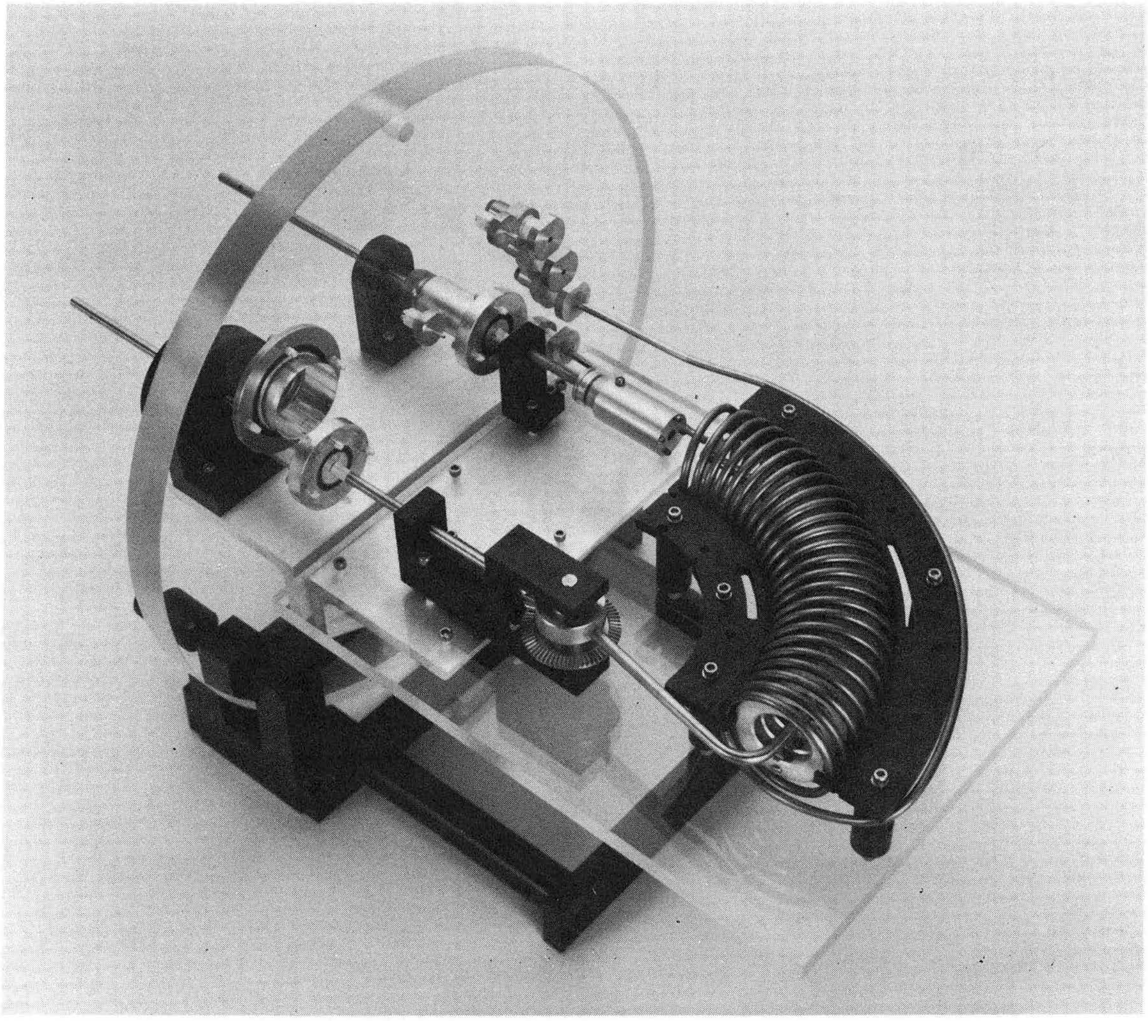

Figure 1(b)

CBB 887-6897

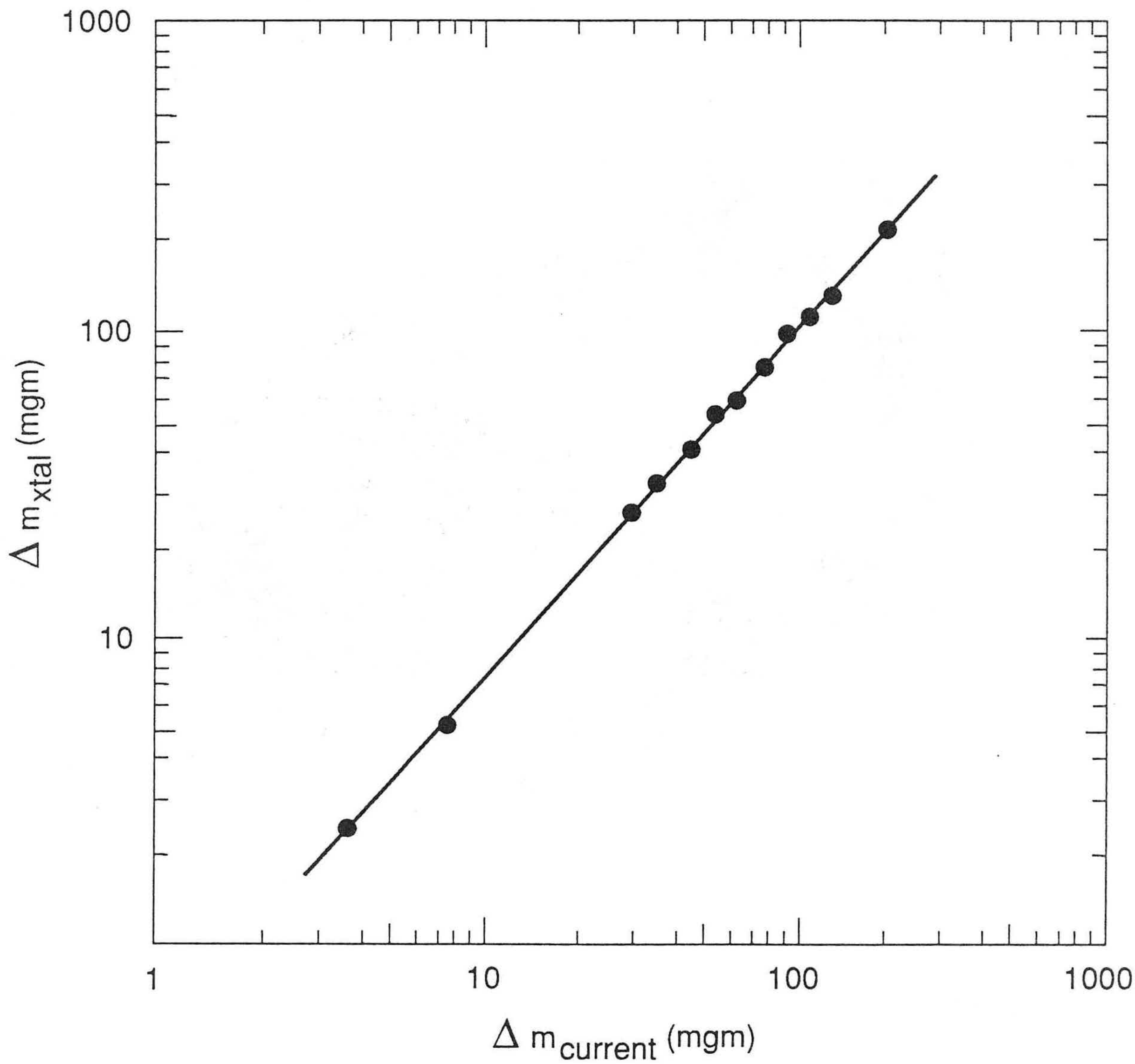

Figure 2

XBL894-6011

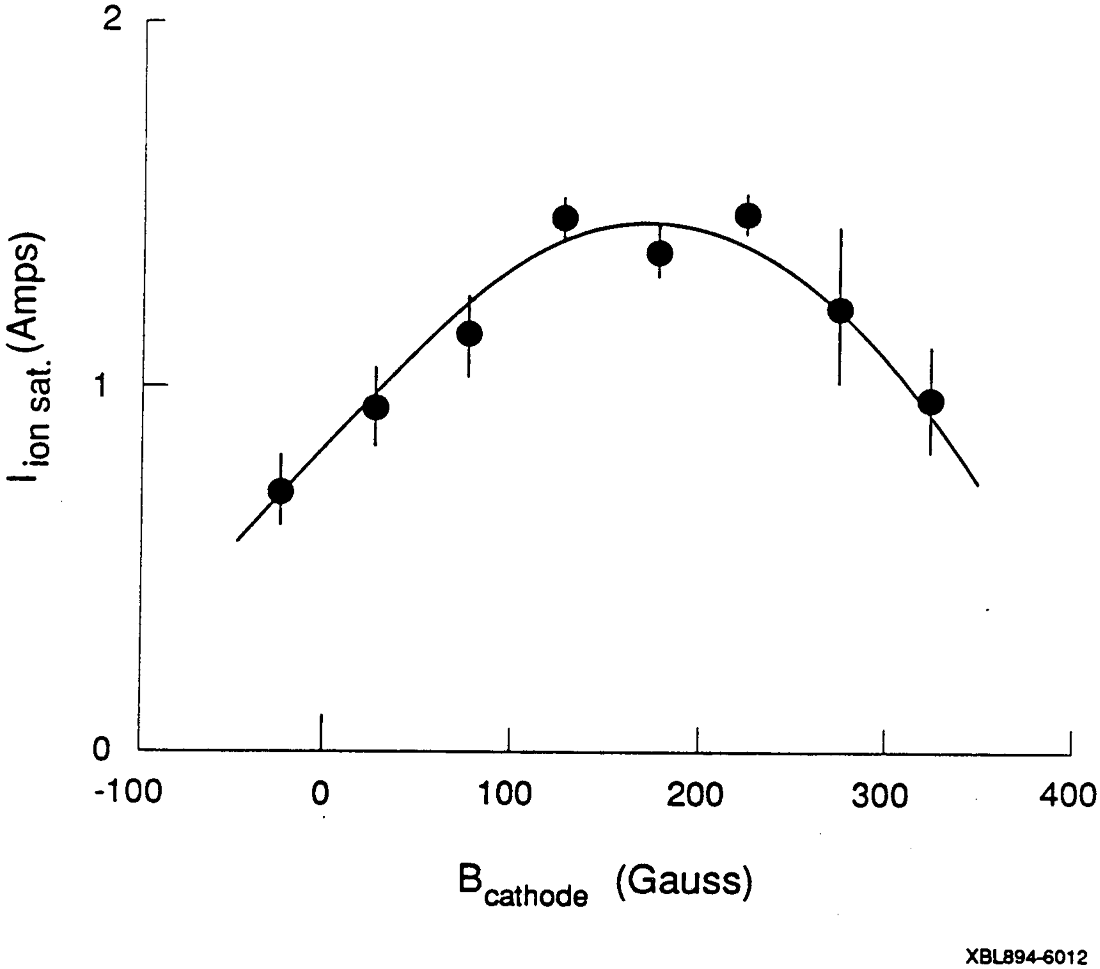
2
1
0
I ion sat. (Amps)
-100
0
100
200
300
400
B cathode (Gauss)
XBL894-6012

Figure 3

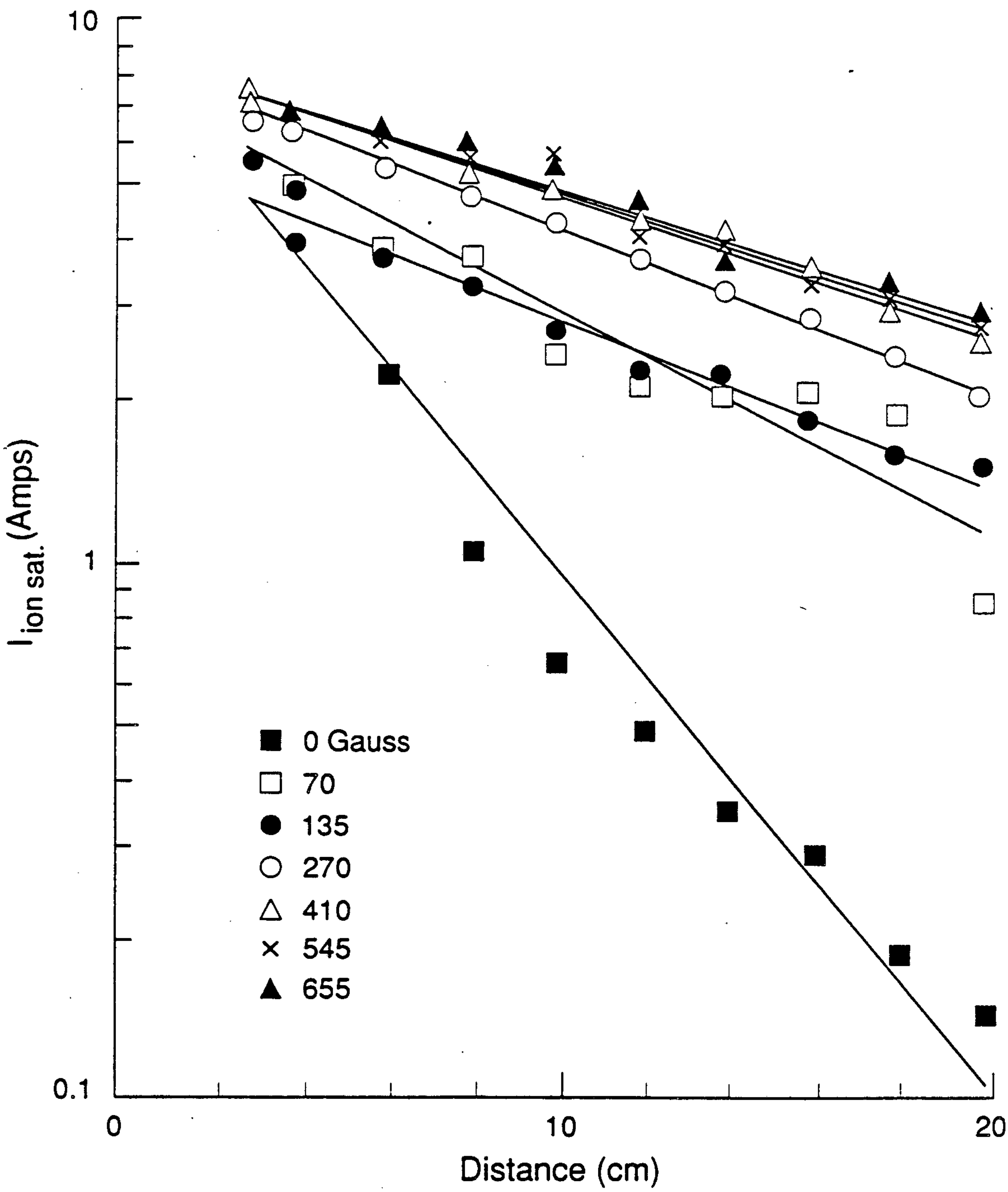
10
1
0.1
$I_{ion\ sat.}$ (Amps)
0
10
20
Distance (cm)
0 Gauss
70
135
270
410
545
655
XBL894-6013

Figure 4

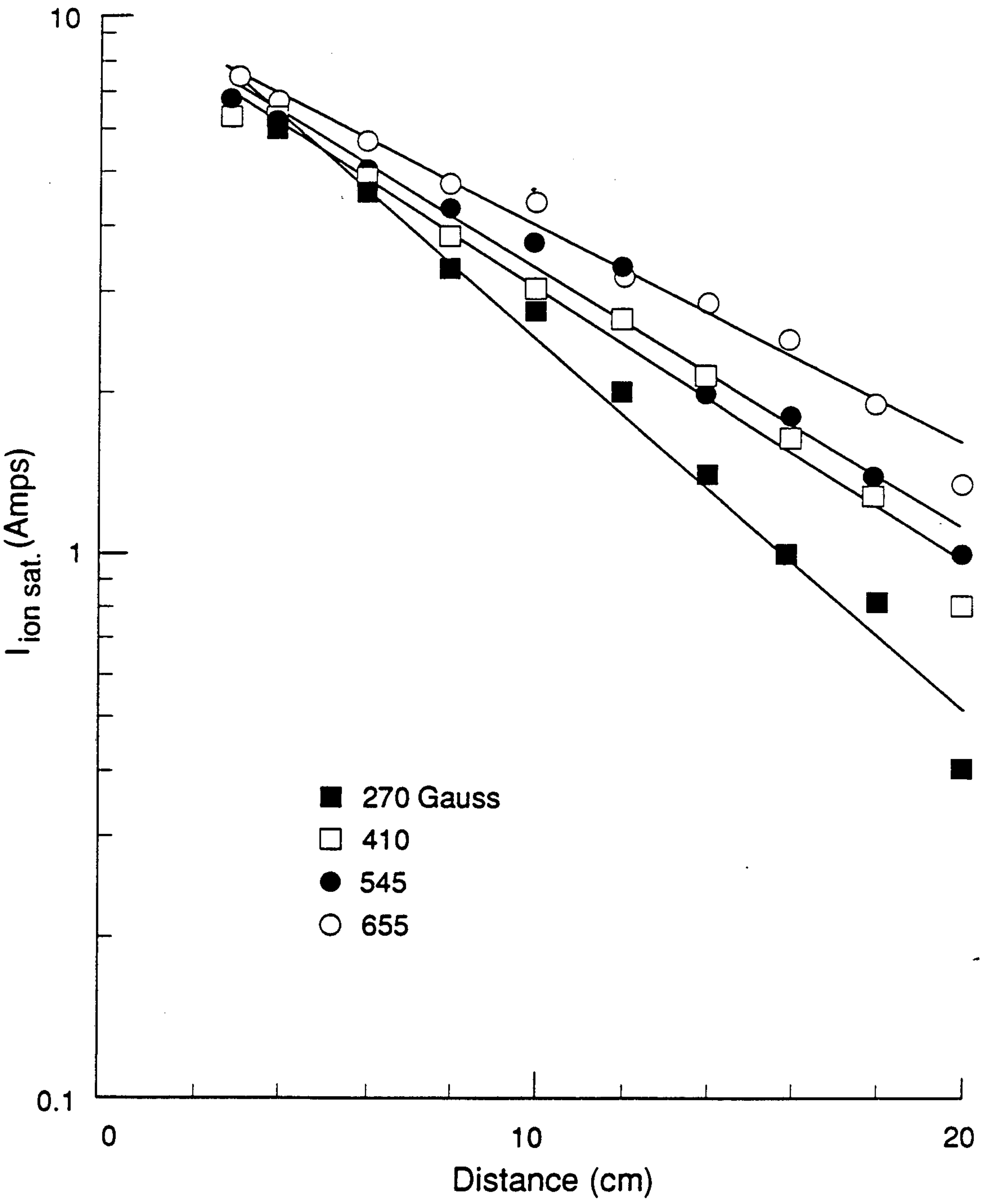

Figure 5

XBL894-6014

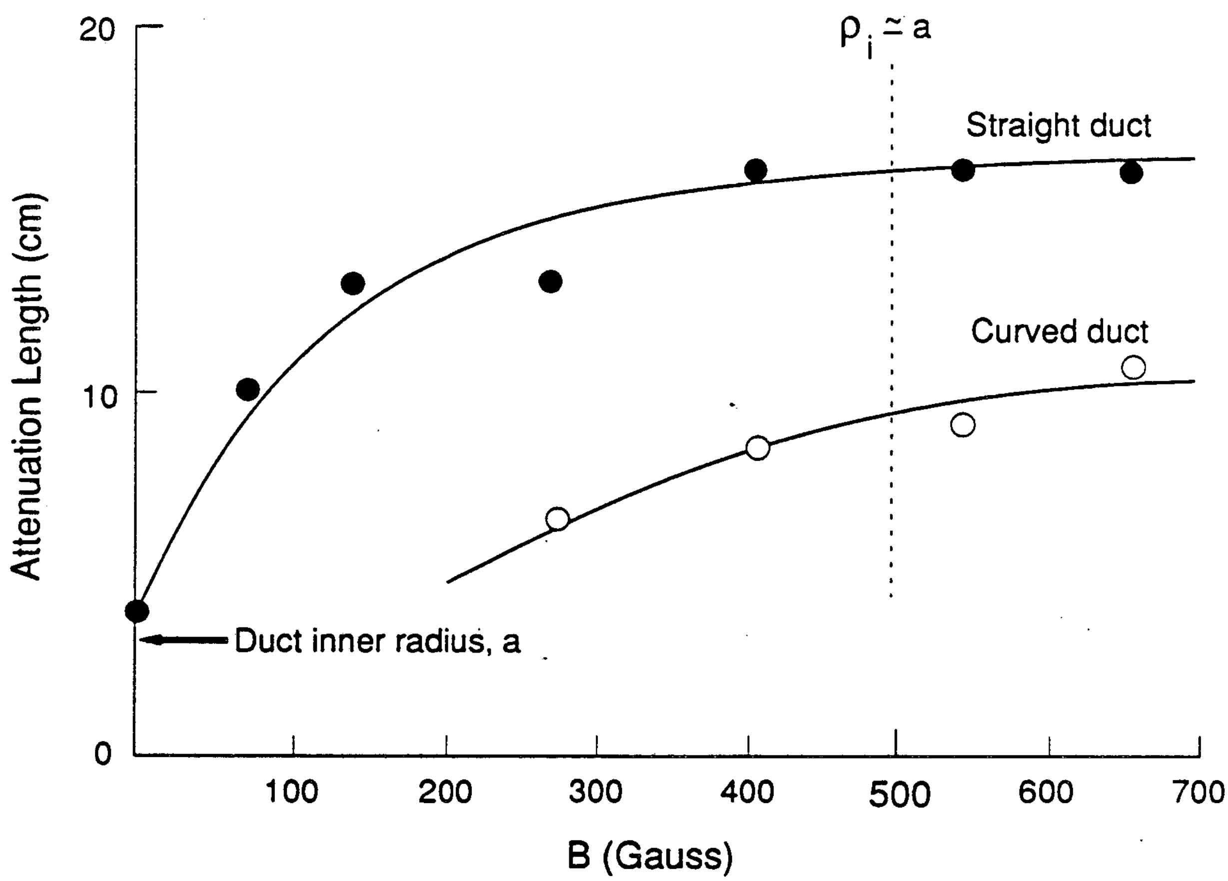

Figure 6

XBL894-6015

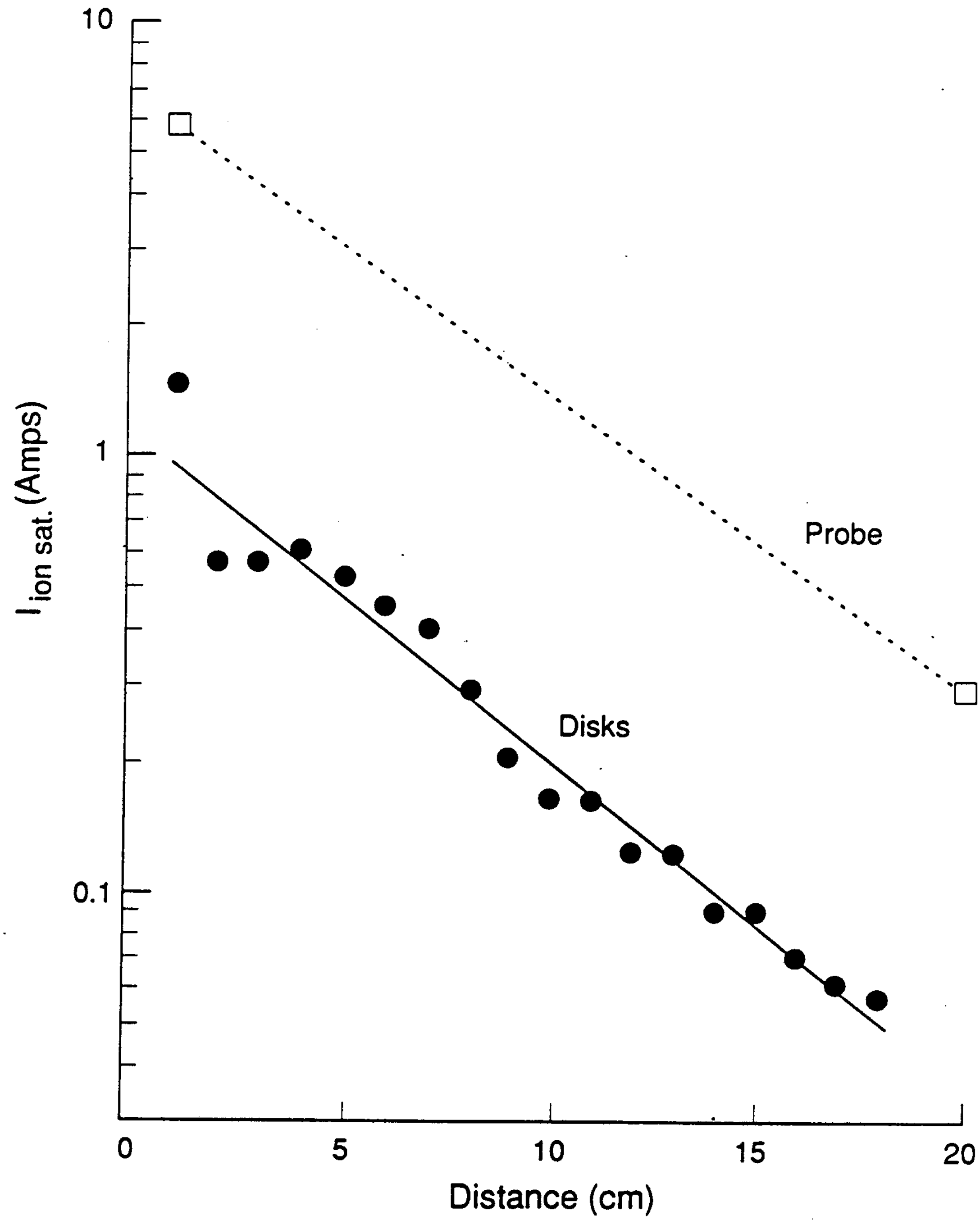

Figure 7

XBL894-6016

LAWRENCE BERKELEY LABORATORY
TECHNICAL INFORMATION DEPARTMENT
1 CYCLOTRON ROAD
BERKELEY, CALIFORNIA 94720